Microenvironment and Immunology

Cancer Research

RETRACTED: Variable Inhibition of Thrombospondin 1 against Liver and Lung Metastases through Differential Activation of Metalloproteinase ADAMTS1

Yoon-Jin Lee[1], Moritz Koch[1], Daniel Karl[1], Antoni X. Torres-Collado[2], Namali T. Fernando[1], Courtney Rothrock[1], Darshini Kuruppu[1], Sandra Ryeom[3], M. Luisa Iruela-Arispe[2], and Sam S. Yoon[3,4]

Abstract

Metastasis relies on angiogenesis for tumor expansion. Tumor angiogenesis is restrained by a variety of endogenous inhibitors, including thrombospondin 1 (TSP1). The principal antiangiogenic activity of TSP1 resides in a domain containing three TSP1 repeats (3TSR), and TSP1 cleavage is regulated, in part, by the metalloproteinase ADAMTS1. In this study, we examined the role of TSP1 and ADAMTS1 in controlling metastatic disease in the liver and lung. TSP1 overexpression inhibited metastatic growth of colon or renal carcinoma cells in liver but not lung. Metastatic melanoma in liver grew more rapidly in *Tsp1*-null mice compared with controls, whereas in lung grew similarly in *Tsp1*-null mice or controls. Recombinant TSP1 was cleaved more efficiently in lysates from liver than lung. ADAMTS1 inhibition by neutralizing antibody, small interfering RNA, or genetic deletion abrogated cleavage activity. To confirm that lack of cleavage of TSP1 ablated its antiangiogenic function in the lung, we generated colon cancer cells stably secreting only the 3TSR domain and found that they inhibited formation of both liver and lung metastases. Collectively, our results indicate that the antiangiogenic activity of TSP1 is differentially regulated by ADAMTS1 in the liver and lung, emphasizing the concept that regulation of angiogenesis is varied in different tissue environments. *Cancer Res; 70(3); 948–56. ©2010 AACR.*

Introduction

Angiogenesis is a dynamic process driven by various proangiogenic factors, including vascular endothelial growth factor-A (VEGF-A or VEGF; refs. 1, 2). However, angiogenesis is also under constant restraint by a variety of endogenous inhibitors, and the modulation of these inhibitors plays a critical role in tumor formation and progression (3). Thrombospondin 1 (TSP1) was the first endogenous angiogenesis inhibitor to be identified (4). TSP1 inhibits angiogenesis by a variety of mechanisms, including suppression of endothelial cell proliferation and migration, inducing endothelial cell apoptosis, and inhibiting growth factor mobilization and access to the endothelial cell surface (5). Lack of TSP1 is associated with increased tumorigenesis in spontaneous tumor models as well as transplantable tumor models (6–8). Overexpression of TSP1 or exogenous administration of TSP1 inhibits tumor formation and progression in several mouse models (9, 10).

The structure of TSP1 has been well characterized and includes three properdin-like repeats or TSP1 repeats (also known as the 3TSR domain; ref. 11). The antiangiogenic activity of TSP1 resides primarily in the 3TSR region, as this domain mediates the interaction of TSP1 with CD36, which is responsible for inducing endothelial apoptosis (3, 12). Recently, we reported that ADAMTS1 cleaves matrix-bound TSP1, releasing the COOH-terminal domain containing the antiangiogenic 3TSR region (13). ADAMTS1 is a matrix metalloproteinase containing TSP1-like domains and is broadly expressed during development and in a variety of adult tissues (14).

The liver and lung are the two most common sites of metastatic disease from solid tumors. In this study, we examined the role of TSP1 in negatively regulating angiogenesis of metastatic tumors in the liver and lung.

Materials and Methods

Plasmids and reagents. Human *Tsp1* cDNA was purchased from Addgene and PCR amplified. The 3TSR fragment was PCR cloned into the plasmid pSecTag2.HygroB (Invitrogen) to create pSecTag2.3TSR, which was sequenced to confirm that

Authors' Affiliations: [1]Department of Surgery, Massachusetts General Hospital and Harvard Medical School, Boston, Massachusetts; [2]Department of Molecular, Cell and Developmental Biology, University of California at Los Angeles, Los Angeles, California; and Departments of [3]Cancer Biology and [4]Surgery, University of Pennsylvania School of Medicine, Philadelphia, Pennsylvania

Note: Supplementary data for this article are available at Cancer Research Online (http://cancerres.aacrjournals.org/).

Y-J. Lee and M. Koch contributed equally to this work.

Corresponding Author: Sam S. Yoon, University of Pennsylvania School of Medicine, 4 Silverstein, 3400 Spruce Street, Philadelphia, PA 19104. Phone: 215-614-0857; Fax: 215-662-7476; E-mail: sam.yoon@uphs.upenn.edu.

doi: 10.1158/0008-5472.CAN-09-3094

no mutations were introduced. Recombinant human ADAMTS1 and TSP1 proteins were purchased from R&D Systems.

Cell lines and tissue culture. CT26 mouse colon carcinoma, RenCa renal carcinoma, and B16F10 mouse melanoma cell lines were obtained from the America Type Culture Collection [American Type Culture Collection (ATCC)]. Cell lines were actively passaged for <6 mo from the time that they were received from ATCC, and United Kingdom Coordinating Committee on Cancer Research guidelines were followed (15). Human umbilical vascular endothelial cells (HUVEC), primary human hepatocytes, human liver sinusoidal endothelial cells, and human lung microvascular endothelial cells were obtained from Lonza.

Generation of stable cell lines expressing TSP1 and 3TSR. TSP1- and 3TSR-secreting CT26 and RenCa cell lines were generated as previously described (16).

Cancer cell and endothelial cell* in vitro *assays. To assay for cancer cell proliferation, 10^4 cells were plated onto 96-well plates. A colorimetric MTT assay was used to assess cell number by absorbance after 1, 3, and 5 d as previously described (16). HUVEC proliferation and migration in response to tumor cell–conditioned medium and liver sinusoidal epithelial cell and lung microvascular epithelial cell proliferation and migration in response to VEGF and TSP1 were performed as previously described (16).

Animal studies. All mouse protocols were approved by the Massachusetts General Hospital Subcommittee on Research Animal Care. To generate subcutaneous flank tumor, 10^6 B16F10 cells were resuspended in 100 μL HBSS and injected s.c. into the right flank of *Tsp1*-null mice or wild-type (WT) littermates (C57BL/6 background) following isoflurane anesthesia. Five mice were used for each group. Tumors were measured thrice per week, and tumor volume (TV) was calculated by using the following formula: TV = length × $(\text{width})^2$ × 0.52. To generate experimental liver and lung metastases, mice were anesthetized using ketamine/xylazine anesthesia, and 5×10^5 to 1×10^6 CT26 cells or RenCa cells resuspended in 100 μL of HBSS were injected intrasplenically or into the tail vein. Five 6- to 8-wk-old male BALB/c mice were used for each group. Mice were sacrificed after 2 wk for liver metastases or 3 wk for lung metastases. Organs were harvested, weighed, fixed in formalin for 24 h, and photographed. Subsequently, organs were embedded in paraffin and processed into 5-μm sections.

To determine number and size of metastases, paraffin-embedded organs were serially sectioned with 0.5 to 1 mm between sections. Two magnified fields per section and five sections per organ were examined, and metastases were counted by a blinded observer. Photos were taken of each counted field and the area of each metastasis was determined using SPOT Advanced v4.6 software (Diagnostic Instruments, Inc.).

Quantitative reverse transcription-PCR. Quantitative real-time-PCR analysis was done using the LightCycler Detection System (Roche Diagnostics) as previously described (16).

Western blot analysis. Western blot analysis for myc was performed as previously described (16). For TSP1 Western blots, two commercial antibodies (2 μg/mL; Ab-4 and Ab-9; NeoMarkers) and two previously described antibodies (Ab#78 and Ab#80) were used (13). Additional Western blots included ADAMTS1 (1:1,000; Santa Cruz Biotechnology), β-actin (1:1,000; Sigma), CD31 (1:500; BD Pharmingen), and CD36 (1:200; Abcam).

***TSP1 cleavage assay* in vitro.** Normal BALB/c mouse liver and lung tissues were harvested and protein lysates were homogenized in radioimmunoprecipitation assay buffer using sonication. Liver and lung tissues were harvested from 6- to 12-wk-old *Adamts1*-null mice or WT littermates and processed in a similar fashion. Recombinant TSP1 (rTSP1) protein (1.5 μg; R&D Systems) was incubated with protein lysates (200 μg) in a buffer containing 50 mmol/L Tris (pH 7.4), 10 mmol/L $CaCl_2$, and 80 mmol/L NaCl for 2 h at 37°C in a maximum volume of 60 μL. The reaction was terminated by adding Laemmli buffer and then resolved on a 10% gradient SDS-PAGE gel. Where indicated, rTSP1 protein was added to protein lysates along with recombinant ADAMTS1 (rADAMTS1) protein (1.5 μg; R&D Systems) and/or anti-ADAMTS1 antibody (1:100; Santa Cruz Biotechnology) and then assayed as described above.

Lentiviral knockdown of ADAMTS1 in liver endothelial cells. Lentiviral constructs for short hairpin RNAs to silence human ADAMTS1 and control lentiviral constructs encoding a scrambled were purchased from Thermo Scientific Dharmacon and include a TurboGFP reporter gene to assess transduction efficiencies.

Cleavage of TSP1 in cell lysates and supernatants of liver endothelial cells. For analysis of TSP1 cleavage by liver and lung endothelial cell lysates, cells were incubated for 48 h following infection by lentiviral constructs. Cells were then split and placed in Opti-MEM (Life Technologies) with 1% fetal bovine serum. After 48 h, conditioned media and cell lysates were harvested separately. rTSP1 protein (1.5 μg) was added to cell lysates (200 μg) and then incubated for 2 h at 37°C.

For analysis of TSP1 cleavage by secreted ADAMTS1 from liver and lung endothelial cells, conditioned media were harvested and then incubated with rTSP1 (1.5 μg) for 4 h at 37°C. Total proteins in conditioned media were precipitated with 10% trichloroacetic acid and incubated at −20°C overnight. After centrifugation at 15,000 × *g* for 10 min, the same volume of cold acetone was added to the precipitated protein pellet and then incubated at −20°C for 10 min. After centrifugation at 15,000 × *g* for 10 min, the protein pellet was air dried and resolubilized in Laemmli buffer.

Immunofluorescence. Paraffin sections were coimmunostained with rat anti–VE-cadherin (1:100; R&D Systems) and mouse anti-ADAMTS1 (1:100; Santa Cruz Biotechnology) or rat anti–VE-cadherin (1:100; R&D Systems) and mouse anti-Tsp1 (1:50; NeoMarkers) overnight at 4°C. Following washing, sections were incubated with goat anti-rat Alexa Fluor 594–conjugated and goat anti-mouse Alexa Fluor 488–conjugated secondary antibodies (1:500; Molecular Probes) at room temperature for 1 h. Images were obtained on Zeiss microscope and analyzed using AxioVision 4.0 software (Carl Zeiss Vision).

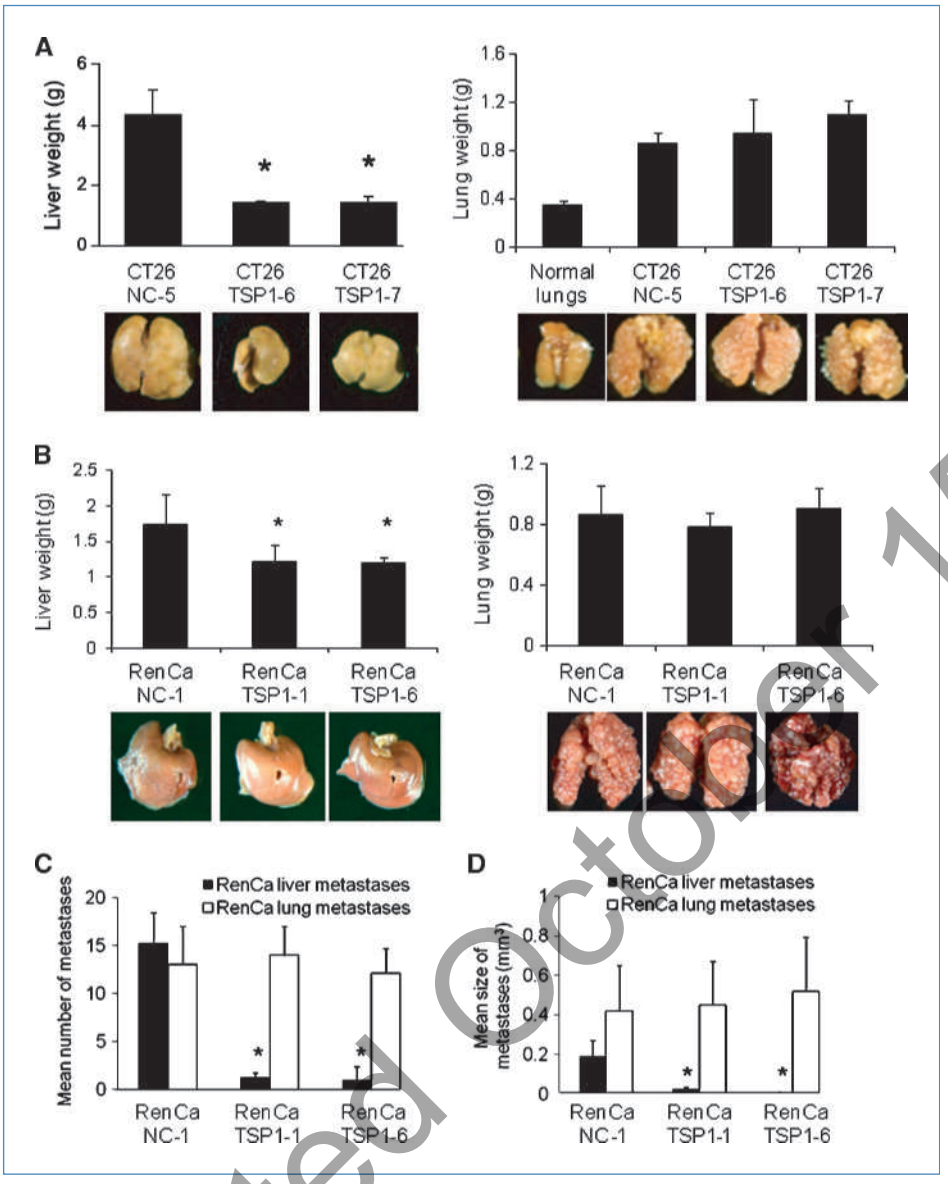

Figure 1. Differential efficacy of TSP1 against liver and lung metastases. A, mean liver and lung weights of organs harvested from mice 14 d after intraportal injection or 21 d after tail vein injection of CT26 control cells (*CT26.NC-5*) or CT26 cells secreting TSP1 (*CT26.TSP1-6* and *CT26.TSP1-7*). Photos of representative organs and weight of normal lungs shown for reference. B, mean weights of livers and lungs harvested from mice after intraportal or tail vein injection of RenCa control cells (*RenCa.NC-1*) or RenCa cells secreting TSP1 (*RenCa.TSP1-1* and *RenCa.TSP1-6*). Mean number (C) and size (D) of RenCa metastases in livers and lungs harvested at 10 d and 14 d, respectively. Bars, SD. *, $P < 0.05$, compared with control group.

Statistical analysis. Groups were compared using Instant 3.10 (GraphPad). For comparisons between three groups (one control group and two treatment groups), treatment groups were compared with the control group using one-way ANOVA with Bonferroni adjustment for multiple comparisons. *P* values of <0.05 were considered significant. Please see Supplementary Materials and Methods for additional information.

Results

Overexpression of TSP1 inhibits growth of CT26 and RenCa liver metastases but not lung metastases. To determine whether upregulation of full-length TSP1 would be sufficient to block the growth of liver or lung metastases, we used murine CT26 colon carcinoma and RenCa renal carcinoma cell lines with stable secretion of TSP1. CT26 cell lines with stable secretion of TSP1 (CT26.TSP1-6 and CT26.TSP1-7), RenCa cell lines with stable secretion of TSP1 (RenCa.TSP1-1 and RenCa.TSP1-6), and negative control cell lines (CT26.NC-5 and RenCa.NC-1) have been previously described (16). These cell lines show equal growth rates *in vitro*, but TSP1-secreting cell lines grow significantly more slowly in the subcutaneous flank region of syngeneic BALB/c mice (compared with the control cell lines) and resulting tumors have decreased microvessel density. When these CT26 cell lines were injected into the portal venous system of syngeneic BALB/c mice to generate experimental liver metastases, TSP1-secreting cell lines formed no visible metastases after 2 weeks, whereas the control cell line formed diffuse, large metastases (Fig. 1A). These same CT26 cell lines were injected into the tail vein of mice to generate lung metastases. Interestingly, secretion of TSP1 from CT26 cells failed to

prevent the growth of CT26 lung metastases. To confirm that *Tsp1* transgene expression was not turned off, we performed immunohistochemistry for the myc tag in lung metastases and found transgene expression throughout CT26.TSP1-6 and CT26.TSP1-7 lung metastases (data not shown).

To ensure that the differential efficacy of TSP1 against the liver and lung metastases was not only specific to the CT26 cell line, we performed similar experiments with stable TSP1-secreting cell lines generated from RenCa cells (16). When these cell lines were injected into the portal venous system, TSP1 was again able to inhibit the growth of liver metastases (Fig. 1B). Diffuse macroscopic liver metastases were visible in mice injected with control cells, whereas no macroscopic liver metastases were visible in mice injected with TSP1-secreting cells, and the mean liver weights of these groups were significantly different. However, when these three RenCa cell lines were used to generate experimental lung metastases, TSP1 secretion again had no effect on the growth of lung metastases. H&E sections of livers again confirmed diffuse small microscopic metastases in RenCa.TSP1-6 and RenCa.TSP1-7 livers compared with significantly larger macroscopic metastases in RenCa.NC-1 livers (Supplementary Fig. S1). We serially sectioned livers and lung with RenCa metastases and found that TSP1 secretion from RenCa cells dramatically decreased both number and size of liver metastases compared with control but made no difference in number or size of lung metastases (Fig. 1C and D).

TSP1 liver and lung metastases in* Tsp1*-null mice. One possible reason that TSP1 inhibits liver metastases but not lung metastases may be due to the significant difference in endogenous levels of TSP1 in the lung and liver. Lawler and colleagues (17) examined RNA levels of TSP1 in the liver and lung using an RNase protection assay and found significantly higher levels of TSP1 in the lung compared with the liver. We confirmed greater levels of TSP1 in normal lung compared with normal liver at the RNA and protein levels using quantitative reverse transcription-PCR (RT-PCR; Fig. 2A) and Western blot analysis (Fig. 2B), respectively. Because endogenous TSP1 levels are already high in the lung microenvironment, additional secretion of TSP1 by cancer cells may not offer any additive antiangiogenic surveillance. We sought to explore this hypothesis by examining liver and lung metastases in *Tsp1*-null mice (*Tsp1*$^{-/-}$). Given *Tsp1*-null mice were obtained in a C57BL/6 background, we used syngeneic B16F10 melanoma cells to generate flank tumors in these mice and in littermate controls. As seen in earlier studies (6), B16F10 cells formed larger flank tumors in *Tsp1*-null mice compared with WT mice (Fig. 2C). Furthermore, when B16F10 experimental liver metastases were generated, B16F10 cells formed generally larger liver metastases in *Tsp1*-null mice compared with control mice ($P = 0.047$; Fig. 2D). However, when B16F10 experimental lung metastases were examined, B16F10 cells formed equivalent lung metastases in *Tsp1*-null mice compared with control mice

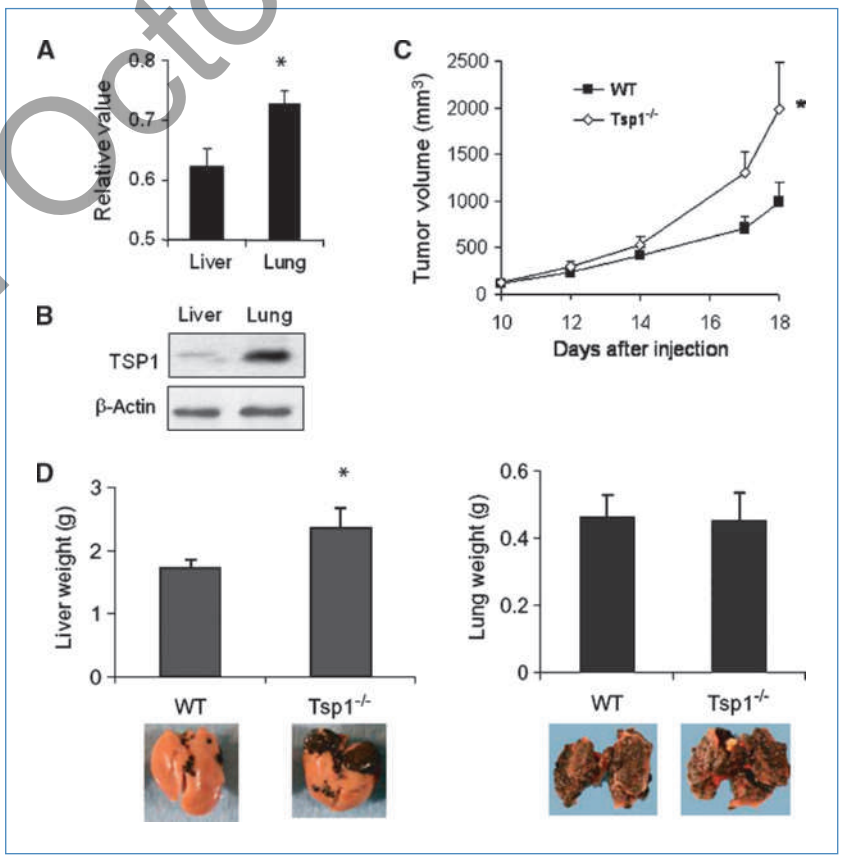

Figure 2. Growth of liver and lung metastases in *Tsp1*-null and WT mice. A, relative levels of *Tsp1* expression in normal mouse liver and lung as measured by quantitative RT-PCR. B, Western blot analysis of TSP1 in normal mouse liver and lung. β-Actin blot serves as loading control. C, flank tumor growth of B16F10 cells in *Tsp1*-null mice (*Tsp1*$^{-/-}$) and WT littermates. D, mean weight of livers and lung harvested from mice 14 d after intraportal injection or 21 d after tail vein injection of B16F10 cells. Bars, SD. *, $P < 0.05$.

($P = 0.91$). Collectively, these studies indicate that the ability of TSP1 to inhibit tumor growth seems to be significantly abrogated in the lung.

Variable efficacy of TSP1 is not due to differences in liver and lung endothelial cells. Alternative hypotheses to the above findings are (*a*) the lung may lack the required receptors for TSP1 to inhibit metastatic tumor growth and (*b*) lung endothelial cells are less sensitive to TSP1. The primary receptor mediating the antiangiogenic effects of TSP1 is CD36 (18). We examined CD36 levels at the protein level in normal liver and lung tissue lysates as well as CT26 liver and lung metastases and found that CD36 levels were actually higher in the normal lung than normal liver and that levels of CD36 in metastases were slightly higher in CT26 lung metastases compared with liver metastases (Fig. 3A). We confirmed these findings by examining lysates of human liver sinusoidal endothelial cells and human lung microvascular endothelial cells (data not shown). We next examined the ability of TSP1 to inhibit proliferation and migration of liver and lung microvascular endothelial cells *in vitro*. TSP1 inhibited VEGF-induced migration similarly in liver sinusoidal endothelial cells and in lung microvascular endothelial cells (Fig. 3B). Of note, TSP1 had no effect on VEGF-induced proliferation of liver and lung endothelial cells (Fig. 3C).

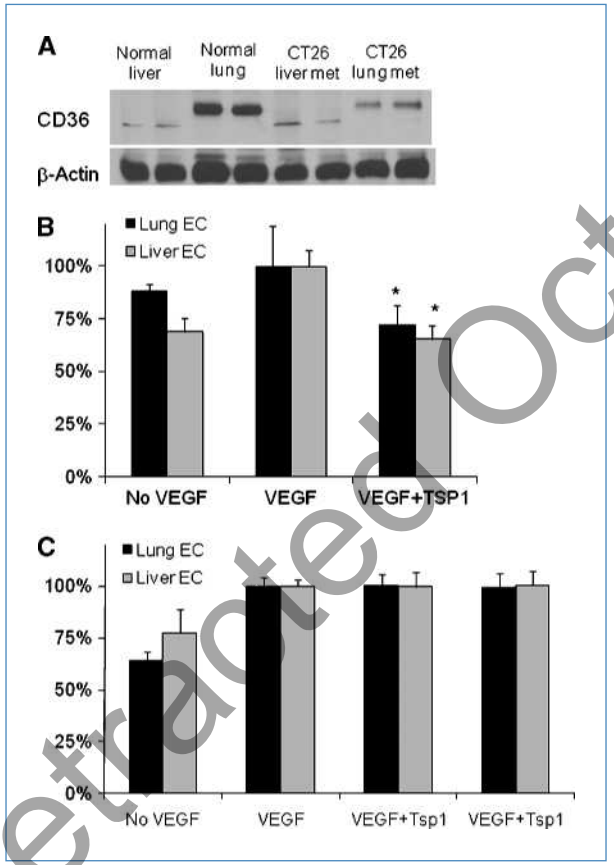

Figure 3. CD36 receptor levels and proliferation/migration of liver and lung endothelial cells *in vitro*. A, Western blot analysis of CD36 levels in normal mouse liver and lung and CT26 liver and lung metastases. B, endothelial cell migration of liver sinusoidal endothelial cells (*Liver EC*) and lung microvascular endothelial cells (*Lung EC*) toward VEGF in a modified Boyden chamber with and without TSP1. *, $P < 0.05$, compared with VEGF alone. C, proliferation of liver EC and lung EC with and without VEGF and TSP1.

ADAMTS1 cleaves TSP1 in the liver. We previously reported that ADAMTS1 can cleave matrix-bound TSP1 and release the COOH-terminal region containing the 3TSR region (13). Thus, we next examined the ability of liver and lung tissue lysates to cleave rTSP1. The careful analysis of TSP1 degradation was made possible by using four different antibodies to TSP1 as shown in Fig. 4A. Ab-4 binds an epitope either in or near the 3TSR domain (19). Ab#80 recognizes only uncleaved TSP1 and Ab#78 recognizes a neoepitope formed after TSP1 is cleaved (13). rTSP1 was cleaved significantly more by liver lysate than by lung lysate (Fig. 4B), suggesting that the liver may have a greater ability to release antiangiogenic fragments of TSP1. In addition, the cleavage pattern observed when rTSP1 was combined with liver lysate was very similar to the cleavage pattern observed when rTSP1 is combined with rADAMTS1 (13). To identify whether ADAMTS1 may be responsible for differential cleavage of TSP1 in the liver and lung, liver or lung tissue lysates were combined with rTSP1 protein, rADAMTS1 protein, and/or neutralizing anti-ADAMTS1 antibody (Fig. 4C). Lung lysate incompletely cleaved rTSP1, this proteolytic activity was greatly increased with the addition of rADAMTS1, and this activity was blocked by anti-ADAMTS1 antibody. Liver lysate alone was sufficient to effectively cleave rTSP1, this activity was not significantly increased with the addition of rADAMTS1, and this activity was blocked by anti-ADAMTS1 neutralizing antibody. These data suggest that the activity of ADAMTS1 in cleaving TSP1 is significantly greater in the liver compared with the lung.

We have previously shown that TSP1 proteolysis is decreased in experimental wounds of *Adamts1*-null mice, resulting in delayed wound healing despite increased angiogenesis (13). We next examined the ability of lung and liver tissue lysates from *Adamts1*-null mice and WT littermates to cleave rTSP1. We probed for TSP1 expression after coincubation of rTSP1 with liver lysates from WT or *Adamts1*-null mice using Ab#80 and Ab#78. Liver lysate from WT mice decreased the amount of uncleaved TSP1 recognized by Ab#80 and increased the amount of cleaved TSP1 recognized by Ab#78 (Fig. 4D). In contrast, liver lysate from *Adamts1*-null mice did not change the amount of uncleaved TSP1 or cleaved TSP1 recognized by Ab#80 and Ab#78, respectively. Lung lysate from both WT mice and *Adamts1*-null mice failed to cleave rTSP1.

We next sought to examine the formation of liver and lung metastases in *Adamts1*-null mice. *Adamts1*-null mice on a mixed 129/Sv × C57BL/6 genetic background exhibit a 40% lethality (20). B16F10 cell lines were created with stable secretion of TSP1, and *Adamts1*-null mice were back bred onto a C57BL/6 genetic background. However, this back breeding led to 100% lethality, and experiments examining B16F10 liver metastases in *Adamts1*-null mice could not be executed.

Knockdown of ADAMTS1 blocks cleavage of TSP1. We next investigated the effect of RNA interference (RNAi) of ADAMTS1 using green fluorescent protein (GFP)–tagged

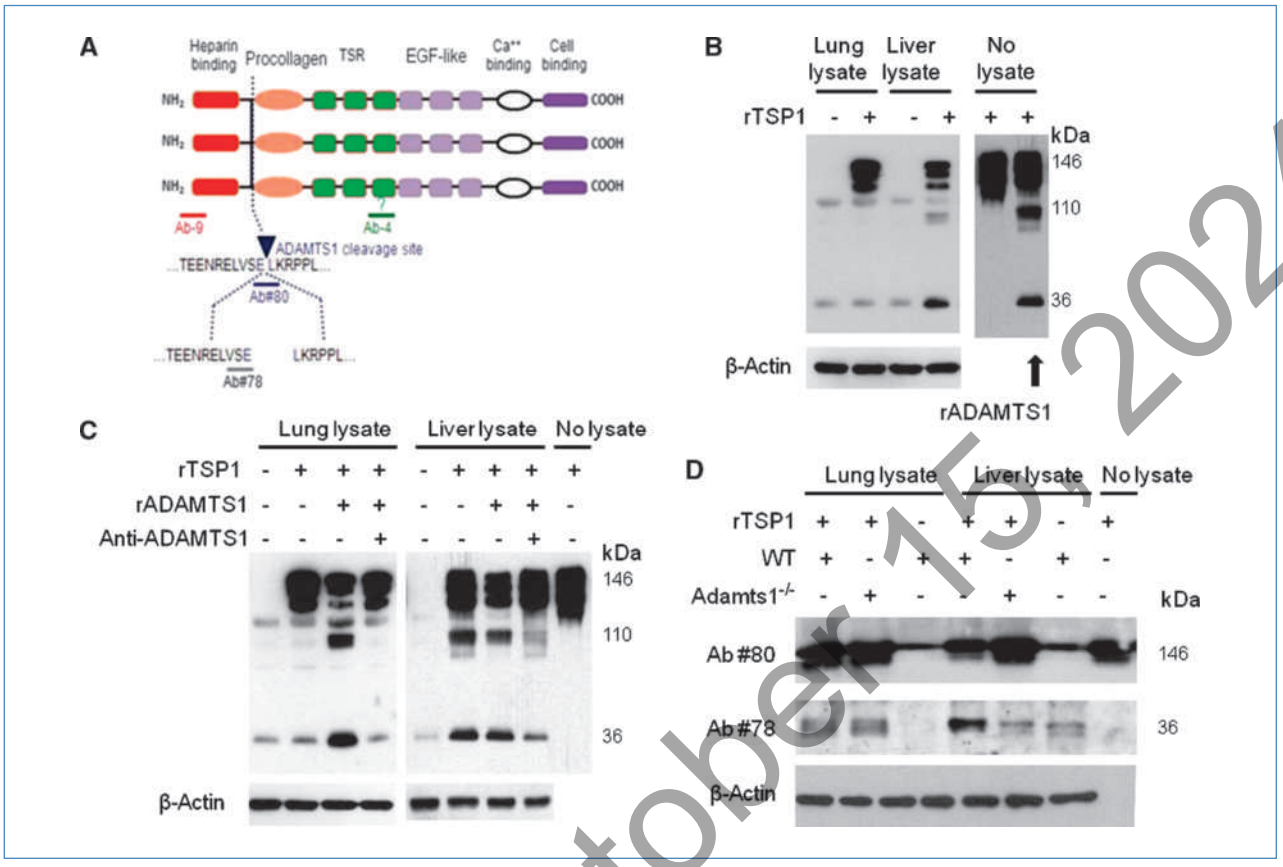

Figure 4. Effect of ADAMTS1 on TSP1 cleavage by liver and lung lysates. A, diagram of antibodies targeting TSP1. B, Western blot of TSP1 following digestion of rTSP1 by normal lung or liver lysate. Also shown is rTSP1 alone (no tissue lysate) and rTSP1 incubated with rADAMTS1. β-Actin Western blot serves as loading control. C, TSP1 Western blot examining digestion of rTSP1 with lung or liver lysate, rADAMTS1, and/or neutralizing ADAMTS1 antibody (*Anti-ADAMTS1*). D, Western blot examining rTSP1 proteolysis by liver or lung lysates from WT mice and *Adamts1*-null mice (*Adamts1*$^{-/-}$).

lentiviral vectors. First, we identified which cell type was the primary endogenous source of TSP1 and ADAMTS1 in the liver. Western blot analysis for TSP1 and ADAMTS1 on primary cultures of cells showed much higher expression of both TSP1 and ADAMTS1 in hepatic sinusoidal endothelial cells and lung microvascular endothelial cells compared with hepatocytes and small airway epithelial cells (Fig. 5A). Coimmunofluorescence of normal mouse liver tissue confirmed that TSP1 and ADAMTS1 colocalized with VE-cadherin, a specific marker of endothelial cells (Fig. 5B). GFP expression showed >90% infection of our RNAi vectors after 48 hours (Supplementary Fig. S2). Infection by either ADAMTS1 lentiviral vector 1 or 2 significantly reduced ADAMTS1 expression as measured by Western blot analysis (Fig. 5C). Cell lysates and supernatants of liver endothelial cells treated with either control lentivirus or anti-ADAMTS1 lentivirus 1 were incubated with rTSP1. Cleavage of rTSP1 was significantly inhibited in liver cell lysates and their respective supernatants following treatment with ADAMTS1 RNAi (Fig. 5D).

Secretion of the antiangiogenic 3TSR fragment of TSP1 inhibits experimental lung metastases. We next determined the effects of the 3TSR domain of TSP1 on liver and lung metastases by generating stable cell lines from CT26 cells. Secretion of the 3TSR protein from two stably transfected cell lines (CT26.3TSR-2 and CT26.3TSR-3) was confirmed by Western blot analysis of conditioned medium (Fig. 6A). The *in vitro* growth rates of CT26.3TSR-2 and CT26.3TSR-3 were equal to the growth rate of the control cell line CT26.NC-5 (Supplementary Fig. S3A), and the secreted 3TSR fragment was also biologically active in abrogating endothelial cell function, as conditioned medium from 3TSR-secreting cell lines inhibited HUVEC proliferation (Fig. 6B).

To confirm the biological activity of the 3TSR fragment in blocking tumor angiogenesis, 3TSR-secreting cells and control cells were grown in the subcutaneous flanks of mice. CT26.3TSR-2 and CT26.3TSR-3 cells formed flank tumors significantly more slowly than CT26.NC-5 cells (Fig. 6C). Microvessel density in tumors from 3TSR-secreting cell lines was significantly decreased compared with CT26.NC-5 control tumors (Supplementary Fig. S3B). When 3TSR-secreting CT26 cells and control CT26 cells were used to generate liver metastases, 3TSR effectively inhibited growth of both liver metastases and lung metastases (Fig. 6D). These data support the notion that the full-length TSP1 protein requires proteolytic degradation to release the 3TSR fragment to inhibit

growth of tumor metastases and that the lung is deficient in this proteolytic activity.

Discussion

This study examined the efficacy of TSP1 against metastases to the liver and lung and found that secretion of TSP1 by cancer cells inhibits the growth of liver metastases but not lung metastases. Furthermore, liver metastases but not lung metastases grow more rapidly in *Tsp1*-null mice compared with WT littermate mice. Liver lysate is much more efficient in cleaving rTSP1 than lung lysate, and the TSP1 cleavage pattern after addition of liver lysate is similar to that seen when TSP1 is cleaved by ADAMTS1. Indeed, neutralizing antibody to ADAMTS1 inhibits the cleavage of TSP1 by liver lysate, liver lysate from *Adamts1*-null mice does not cleave TSP1, and RNAi of ADAMTS1 in liver endothelial cells reduces the ability of these cells to cleave TSP1. When only the 3TSR region is secreted by cancer cells, both liver and lung metastases are inhibited. Thus, the activity of TSP1 against metastases is regulated by cleavage of TSP1 by ADAMTS1, and this proteolytic activity varies according to the host organ environment.

The preferential sites of metastases vary according to the primary tumor. By far, the most common sites of colorectal cancer metastases are the liver and lung (21). Renal cell carcinoma and melanoma can metastasize to many sites, but the liver and lung sites are common (22, 23). Thus, the investigation in this study of liver and lung metastases from these three cancer types is highly clinically relevant. Paget in 1889 proposed his well-known seed and soil hypothesis in which he stated that metastasis was due to the specific affinity of certain tumor cells, or the seeds, to the host organ environment, or the soil (24). There are numerous factors related to the metastasizing cancer cells and the host organ environment, which ultimately determine the development of macroscopic metastases. To our knowledge, this is the first study to examine the variable efficacy of TSP1 against solid organ metastases to different metastatic sites.

In our study, the efficacy of TSP1 in inhibiting liver metastases was independent of the cellular source of TSP1. Thus, cancer cell secretion of TSP1 reduced liver metastases, and host organ loss of TSP1 (as occurs in *Tsp1*-null mice) increased liver metastases. In contrast, there was no effect from TSP1 secretion from cancer cells or from host organ loss of TSP1 on lung metastases. We identified differential ADAMTS1 activity in cleaving TSP1 as an

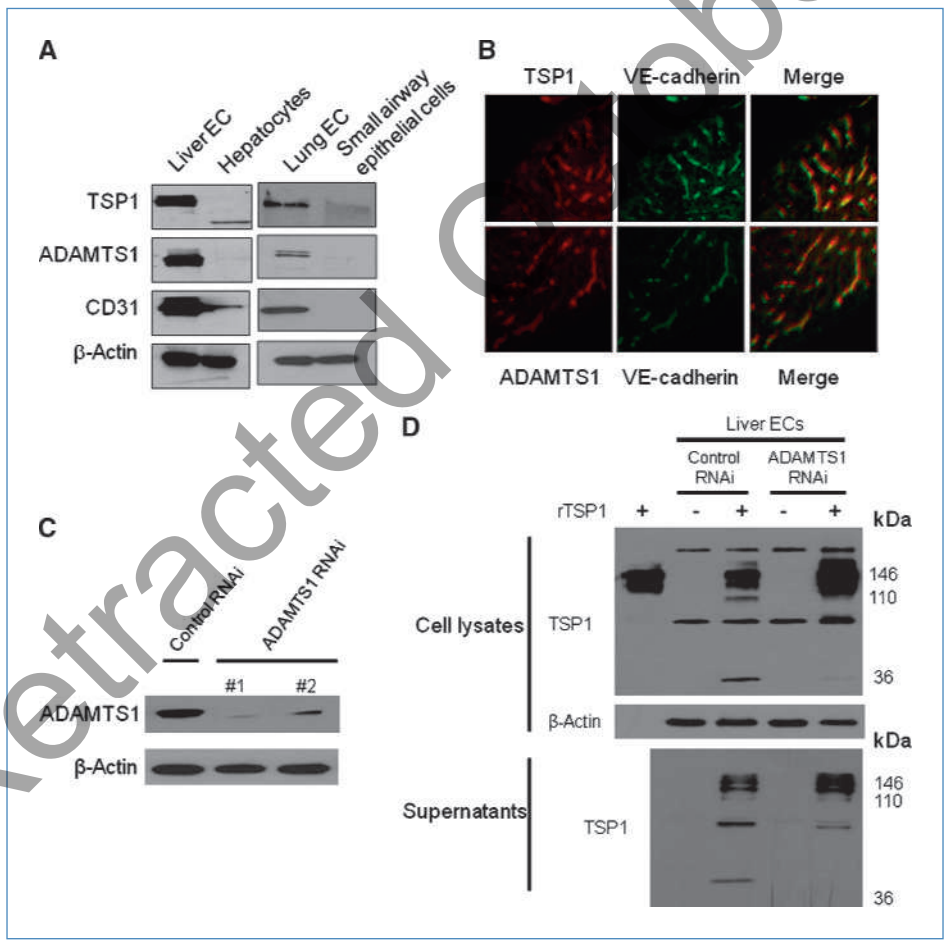

Figure 5. Effect of ADAMTS1 knockdown on TSP1 cleavage. A, Western blot of TSP1, ADAMTS1, CD31, and β-actin in human liver sinusoidal endothelial cells (*Liver EC*), hepatocytes, human lung microvascular endothelial cells (*Lung EC*), and small airway epithelial cells. B, coimmunofluorescence for TSP1 (red), ADAMTS1 (red), and/or VE-cadherin (green) in mouse liver tissue. C, Western blot of ADAMTS1 following infection with ADAMTS1 RNAi lentiviral vectors and control vector. D, Western blot of TSP1 of liver EC lysates (top) and supernatants (bottom) following infection with control lentiviral vector and ADAMTS1 lentiviral vector 1. Lysates or supernatants were incubated with or without rTSP1 protein. Top, left lane, loaded with rTSP1 alone.

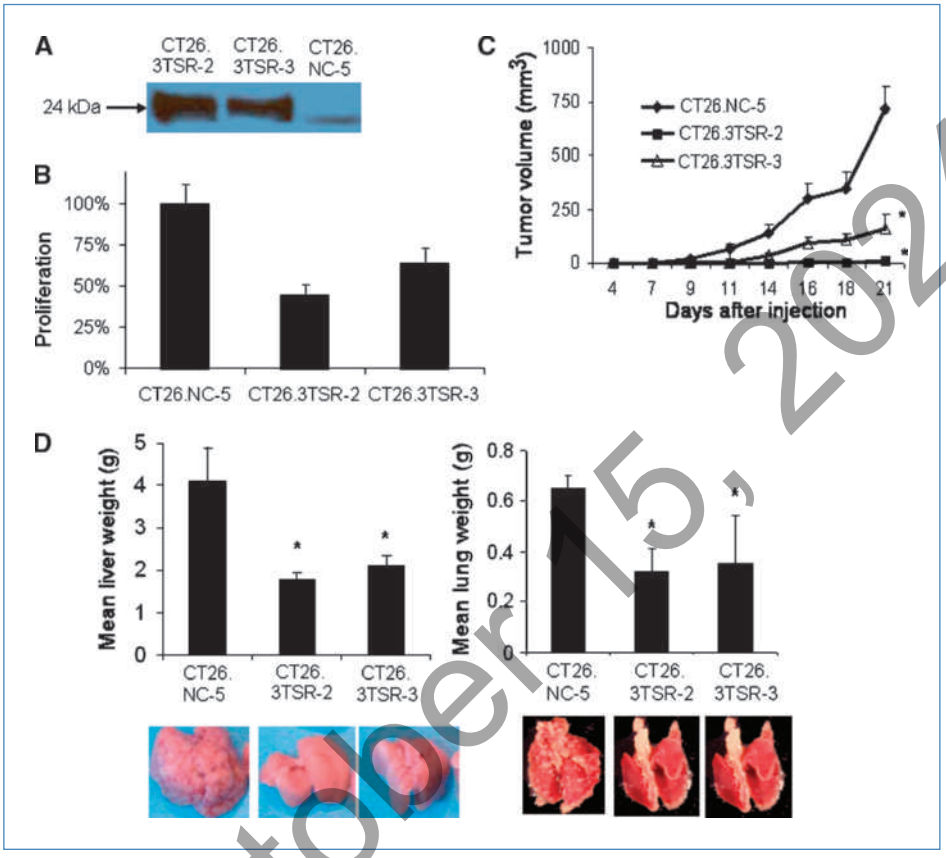

Figure 6. Efficacy of 3TSR against liver and lung metastases. A, Western blot analysis for myc tag of conditioned medium from CT26 cell lines stably oversecreting 3TSR (*CT26.3TSR-2* and *CT26.3TSR-3*) as well as CT26-negative control cell line (*CT26.NC-5*). B, inhibition of HUVEC proliferation with conditioned medium from CT26 cells stably expressing 3TSR. C, flank tumor growth of CT26 cell lines in BALB/c mice. D, mean liver and lung weights of organs harvested from mice after intraportal or tail vein injection of 3TSR-secreting CT26 cell lines compared with control cell line. Bars, SD. *, $P < 0.05$, compared with CT26.NC-5.

explanation for the variable effect of TSP1 against liver and lung metastases, but this differential activity of ADAMTS1 is not due to higher levels of ADAMTS1 in the liver. In fact, ADAMTS1 levels as measured by quantitative RT-PCR are 3- to 4-fold higher in the lung compared with the liver (Supplementary Fig. S2A and B). Thus, we hypothesize that there are inhibitors of ADAMTS1 activity in the lung. We previously examined the ability of tissue inhibitor of metalloproteinase (TIMP) 1 to TIMP4 in inhibiting ADAMTS1 and found TIMP2 and TIMP3 could partially inhibit ADAMTS1 activity, but TIMP1 and TIMP4 had no effect (25). As a preliminary study, we examined levels of TIMP2 and TIMP2 by quantitative RT-PCR and found them to be up to 11-fold higher in the lung compared with the liver (Supplementary Fig. S2A and B).

Interestingly, the primary endogenous source of TSP1 and ADAMTS1 in both the liver and the lung is the microvascular endothelial cells rather than parenchymal cells such as hepatocytes and small airway epithelial cells (Fig. 5). Thus, angiogenic regulation of liver and lung endothelial cells by TSP1 and ADAMTS1 can occur in an autocrine fashion, whereby TSP1 and ADAMTS1 are secreted by the endothelial cells, ADAMTS1 cleaves TSP1 releasing antiangiogenic fragments from the extracellular matrix, and these fragments in turn act locally to inhibit angiogenesis.

We explored alternative explanations for the variable efficacy of TSP1 against liver and lung metastases. Full-length TSP1 was found to have equal efficacy *in vitro* against microvascular endothelial cells isolated from the liver and lung in terms of inhibiting migration, but variable efficacy against these endothelial cells *in vivo* is difficult to study. TSP1 has a variety of functions other than inhibiting angiogenesis (26), and thus, there may be nonangiogenic mechanisms that explain the variable efficacy of TSP1 in different host organ environments. For example, TSP1 can activate transforming growth factor-β, which can either inhibit or stimulate tumor growth and metastasis (27). One of the primary mechanisms by which the 3TSR region inhibits endothelial cells is by binding the scavenger receptor CD36, which induces caspase-dependent apoptosis (12, 28). We found that CD36 levels were higher in lung than liver and that lung and liver endothelial cells were equally responsive to TSP1 inhibition of migration (Fig. 3). Thus, the differences in the efficacy of TSP1 against liver and lung metastases were not explained by differential receptor levels or sensitivity of host organ endothelial cells to TSP1.

In summary, the activity of TSP1 is regulated by extracellular proteases such as ADAMTS1 (29). Given the content and activity of extracellular proteases vary in different organ environments, it is not too surprising that ADAMTS1 regulation of TSP1 activity is markedly different in the liver and lung. Processing of TSP1 into antiangiogenic fragments by ADAMTS1 occurs much more efficiently in the liver, and thus, overexpression of TSP1 in the liver suppresses the vascularization of liver metastases. ADAMTS1 activity is deficient in the lung, and thus, TSP1 overexpression does little to inhibit the vascularization of lung metastases. As TSP1 and other

antiangiogenic therapies move forward in clinical trials for the treatment and possibly prevention of tumors and metastases, differences in the activity and efficacy of these agents in various organ environments should be considered.

Disclosure of Potential Conflicts of Interest

No potential conflicts of interest were disclosed.

Grant Support

NIH grants 5 K12 CA 87723-03 (S.S. Yoon) and 1 R21 CA117129-01 (S.S. Yoon), Polsky Family MGH Junior Faculty (S.S. Yoon), and Jung Foundation for Science and Research (Hamburg, Germany; M. Koch).

The costs of publication of this article were defrayed in part by the payment of page charges. This article must therefore be hereby marked *advertisement* in accordance with 18 U.S.C. Section 1734 solely to indicate this fact.

Received 8/19/09; revised 11/9/09; accepted 11/30/09; published OnlineFirst 1/26/10.

References

1. Ferrara N. Vascular endothelial growth factor. Arterioscler Thromb Vasc Biol 2009;29:789–91.
2. Claesson-Welsh L. Signal transduction by vascular endothelial growth factor receptors. Biochem Soc Trans 2003;31:20–4.
3. Nyberg P, Xie L, Kalluri R. Endogenous inhibitors of angiogenesis. Cancer Res 2005;65:3967–79.
4. Good DJ, Polverini PJ, Rastinejad F, et al. A tumor suppressor-dependent inhibitor of angiogenesis is immunologically and functionally indistinguishable from a fragment of thrombospondin. Proc Natl Acad Sci U S A 1990;87:6624–8.
5. Lawler J, Detmar M. Tumor progression: the effects of thrombospondin-1 and -2. Int J Biochem Cell Biol 2004;36:1038–45.
6. Lawler J, Miao WM, Duquette M, Bouck N, Bronson RT, Hynes RO. Thrombospondin-1 gene expression affects survival and tumor spectrum of p53-deficient mice. Am J Pathol 2001;159:1949–56.
7. Gutierrez LS, Suckow M, Lawler J, Ploplis VA, Castellino FJ. Thrombospondin 1—a regulator of adenoma growth and carcinoma progression in the APC(Min/+) mouse model. Carcinogenesis 2003;24:199–207.
8. Rodriguez-Manzaneque JC, Lane TF, Ortega MA, Hynes RO, Lawler J, Iruela-Arispe ML. Thrombospondin-1 suppresses spontaneous tumor growth and inhibits activation of matrix metalloproteinase-9 and mobilization of vascular endothelial growth factor. Proc Natl Acad Sci U S A 2001;98:12485–90.
9. Hawighorst T, Oura H, Streit M, et al. Thrombospondin-1 selectively inhibits early-stage carcinogenesis and angiogenesis but not tumor lymphangiogenesis and lymphatic metastasis in transgenic mice. Oncogene 2002;21:7945–56.
10. Miao WM, Seng WL, Duquette M, Lawler P, Laus C, Lawler J. Thrombospondin-1 type 1 repeat recombinant proteins inhibit tumor growth through transforming growth factor-β-dependent and -independent mechanisms. Cancer Res 2001;61:7830–9.
11. Carlson CB, Lawler J, Mosher DF. Structures of thrombospondins. Cell Mol Life Sci 2008;65:672–86.
12. Jimenez B, Volpert OV, Crawford SE, Febbraio M, Silverstein RL, Bouck N. Signals leading to apoptosis-dependent inhibition of neovascularization by thrombospondin-1. Nat Med 2000;6:41–8.
13. Lee NV, Sato M, Annis DS, et al. ADAMTS1 mediates the release of antiangiogenic polypeptides from TSP1 and 2. EMBO J 2006;25:5270–83.
14. Thai SN, Iruela-Arispe ML. Expression of ADAMTS1 during murine development. Mech Dev 2002;115:181–5.
15. UKCCCR guidelines for the use of cell lines in cancer research. Br J Cancer 2000;82:1495–509.
16. Fernando NT, Koch M, Rothrock C, et al. Tumor escape from endogenous, extracellular matrix-associated angiogenesis inhibitors by up-regulation of multiple proangiogenic factors. Clin Cancer Res 2008;14:1529–39.
17. Lawler J, Sunday M, Thibert V, et al. Thrombospondin-1 is required for normal murine pulmonary homeostasis and its absence causes pneumonia. J Clin Invest 1998;101:982–92.
18. Silverstein RL, Febbraio M. CD36-TSP-HRGP interactions in the regulation of angiogenesis. Curr Pharm Des 2007;13:3559–67.
19. Ali NA, Gaughan AA, Orosz CG, et al. Latency associated peptide has *in vitro* and *in vivo* immune effects independent of TGF-β1. PLoS One 2008;3:e1914.
20. Shindo T, Kurihara H, Kuno K, et al. ADAMTS-1: a metalloproteinase-disintegrin essential for normal growth, fertility, and organ morphology and function. J Clin Invest 2000;105:1345–52.
21. Libutti SA, Saltz LB, Tepper JE. Colon cancer. In: DeVita VT, Lawrence TS, Rosenberg SA, editors. Cancer: principles and practice of oncology. 8th ed. Philadelphia: Lippincott Williams & Wilkins; 2008, p. 1232–84.
22. Linehan WM, Rini BI, Yang JC. Cancer of the kidney. In: DeVita VT, Lawrence TS, Rosenberg SA, editors. Cancer: principles and practice of oncology. 8th ed. Philadelphia: Lippincott Williams & Wilkins; 2008, p. 1331–57.
23. Slingluff CL, Flaherty K, Rosenberg SA, Reed PW. Cutaneous melanoma. In: DeVita VT, Lawrence TS, Rosenberg SA, editors. Cancer: principles and practice of oncology. 8th ed. Philadelphia: Lippincott Williams & Wilkins; 2008, p. 1897–950.
24. Paget S. The distribution of secondary growths in cancer of the breast. Lancet 1889;1:571–3.
25. Rodriguez-Manzaneque JC, Westling J, Thai SN, et al. ADAMTS1 cleaves aggrecan at multiple sites and is differentially inhibited by metalloproteinase inhibitors. Biochem Biophys Res Commun 2002;293:501–8.
26. Ren B, Yee KO, Lawler J, Khosravi-Far R. Regulation of tumor angiogenesis by thrombospondin-1. Biochim Biophys Acta 2006;1765:178–88.
27. Roberts AB, Wakefield LM. The two faces of transforming growth factor β in carcinogenesis. Proc Natl Acad Sci U S A 2003;100:8621–3.
28. Dawson DW, Pearce SF, Zhong R, Silverstein RL, Frazier WA, Bouck NP. CD36 mediates the *In vitro* inhibitory effects of thrombospondin-1 on endothelial cells. J Cell Biol 1997;138:707–17.
29. Iruela-Arispe ML. Regulation of thrombospondin1 by extracellular proteases. Curr Drug Targets 2008;9:863–8.